Investigations of cosmic rays above the knee by means of muon bundles detected in the wide zenith angle interval

N. S. Barbashina, A. G. Bogdanov, D. V. Chernov, A. N. Dmitrieva, D. M. Gromushkin, V. V. Kindin, R. P. Kokoulin, K. G. Kompaniets, G. Mannocchi, A. A. Petrukhin, O. Saavedra, V. V. Shutenko, D. A. Timashkov, G. Trinchero, I. I. Yashin

***Abstract*— Experimental data on muon bundles at large zenith angles obtained with a large area Russian-Italian coordinate detector DECOR are analyzed in terms of a new phenomenological variable - local density of EAS muons at the observation point. Detector-independent spectra of local muon density are reconstructed from the measured distributions of muon bundle characteristics and are compared with CORSIKA based simulations in zenith angle range from 30° to horizon. It is shown that muon density spectra are sensitive to the primary spectrum shape and primary composition and allow to infer a new information on combinations of these parameters in the energy range $10^{15} – 10^{19}$ eV.**

I. Introduction

EXPERIMENTAL situation with studies of primary cosmic ray characteristics in UHE region is rather controversial. For quantitative interpretation of EAS observation results in this energy range, an adequate knowledge of the expected EAS characteristics is required. Whereas electromagnetic interactions in EAS are well understood, considerable uncertainties exist in the description of hadronic interactions. As a consequence, conclusions on primary spectrum and composition inferred from EAS observations appear model dependent. Therefore, careful validation of calculation results on a basis of the comparison with the available data on different EAS observables in a maximal possible range of their variation is important.

In the present paper, experimental data on muon bundles registered at the Earth's surface in a wide range of zenith angles by means of the large area coordinate detector DECOR [1,2] are analysed in terms of a new EAS observable – local muon density at the observation point. At large zenith angles, typical distances of substantial changes of muon lateral distribution function are hundreds – thousands meters, therefore the detector with dimensions of the order of tens meters may be considered as a point-like probe. In a first approximation, the local muon density D (number of muons per unit area) in the event is estimated as the ratio of the number m of muons that hit the detector (muon bundle multiplicity) to the effective detector area S in a given direction. Contribution to the flux of the events with a fixed local density is given by the showers with different primary energies detected at different random distances from the shower axis; however, due to a fast decrease of the cosmic ray flux with the increase of energy, the effective interval of primary particle energies appears relatively narrow.

Preliminary data concerning the analysis of muon bundles detected in DECOR in frame of the local muon density approach have been presented elsewhere [3,4]. In particular, it was shown that due to a fast variation of the thickness of the atmosphere and distances from generation level to the observation point with zenith angle the data obtained in this experiment correspond to a very wide interval of primary particle energies. Important advances in the results presented here are increased experimental statistics and consideration of the Earth magnetic field (EMF) effect in calculations of expected distributions.

General scheme used in the present analysis includes the following steps: selection of muon bundle events and construction of distributions in muon bundle multiplicity, zenith and azimuth angles; iterative deconvolution of the measured distributions to detector-independent spectra of local muon density for several zenith angle intervals; simulation of muon lateral distribution functions (LDF) for different types of primary particles, energies, and hadronic interaction models by means of the CORSIKA code [5]; calculation of the expected local muon density distributions by means of the convolution of LDF with a certain primary spectrum and composition model; comparison between experimental and calculation results.

II. Experimental

Data collected during long-term experimental runs (14767 hours live time) with the NEVOD-DECOR complex in 2002 – 2005 have been used for the present analysis. A general layout of the setup is shown in Fig.1. The coordinate detector

The research is supported by Russian Federal Agency for Education, Federal Agency for Science and Innovations, and RFBR (grant 06-02-17000a).

N. S. Barbashina, A. G. Bogdanov, D. V. Chernov, A. N. Dmitrieva, D. M. Gromushkin, V. V. Kindin, R. P. Kokoulin, K. G. Kompaniets, A. A. Petrukhin, V. V. Shutenko, D. A. Timashkov, I. I. Yashin are with Moscow Engineering Physics Institute (State University), 115409 Moscow, Russia; e-mail: RPKokoulin@mephi.ru.

G. Mannocchi, G. Trinchero are with Istituto Nazionale di Astrofisica, Sezione di Torino, 10133 Torino, Italy.

O. Saavedra is with Dipartimento di Fisica Generale dell Universita di Torino, 10125 Torino, Italy.

DECOR [1,2] represents a modular multi-layer system of plastic streamer tube chambers with resistive cathode coating, arranged around the Cherenkov water calorimeter NEVOD [6] with sizes $9 \times 9 \times 26$ m^3 and a spatial lattice of quasispherical optical modules. The side part of DECOR includes eight 8-layer assemblies (supermodules, SM) of chambers with the total sensitive area 70 m^2. Chamber planes are equipped with two-coordinate external strip readout system that allows to localize charged particle track with about 1 cm accuracy in both coordinates (X,Y). The distance between the adjacent planes of the supermodule is 6 cm. Angular accuracy of reconstruction of muon tracks crossing the SM is better than 0.7° and 0.8° for projected zenith and azimuth angles, respectively. The permanent component of the Earth magnetic field at the setup location is 52 μT; magnetic inclination 71°.

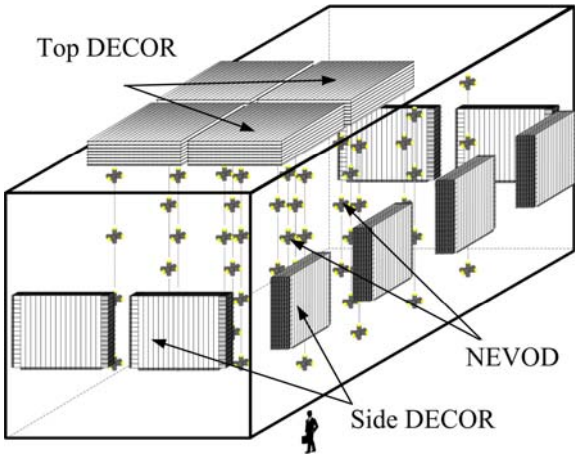

Figure 1. General layout of NEVOD-DECOR complex.

Selection of muon bundle events is based on the assumption that tracks of muons produced in the upper atmosphere (far from the setup) are nearly parallel [7]. The selection procedure includes several stages: trigger selection (coincidence of signals from any three SM of the side part of DECOR); soft program selection of events with quasi-parallel (within 5° cone) tracks; scanning of muon bundle candidates, final event classification, and track counting by operators with the help of a specialized computer interface.

At large angles, EAS reach the setup practically as pure muon component. In these conditions muon bundle events have a very bright signature in the coordinate detector, and their interpretation is unambiguous (Fig.2). However, at lower zenith angles the events are often accompanied by soft EAS component that complicates geometry reconstruction and muon bundle selection. In order to extend the range of measurements to moderate zenith angles and low multiplicities (and, correspondingly, to lower primary energies), for angles less than 75° an additional cut is applied, namely, only events in two limited sectors of azimuth are retained where most of side DECOR supermodules (six of eight) are screened by the water volume of Cherenkov calorimeter, data only of these shielded SM being taken into consideration. Such approach gave possibility to select muon bundles starting from 30° and from a minimal multiplicity determined by trigger conditions ($m \geq 3$).

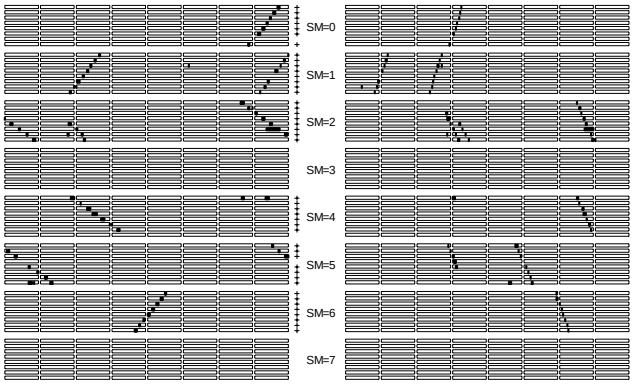

Figure 2. Example of muon bundle event in the coordinate detector (9 parallel tracks, 78° zenith angle). Dark points represent hit strips. Left: Y-coordinate strips of SM (azimuth angle); right: X-coordinate strips (projected zenith angle).

Since the procedure of the bundle selection by the operators is toilsome, and the number of bundles in different multiplicity and zenith angle intervals differs by the orders of magnitude, experimental data are analysed part by part, for separate ranges of m and θ. Statistics of muon bundles of different categories used in the further analysis are summarised in Table I.

TABLE I
STATISTICS OF MUON BUNDLE EVENTS.

m	θ	Time, h	No. events
≥ 3	30° – 40°	250	2258
≥ 3	40° – 60°	250	3748
≥ 3	≥ 60°	758	1928
≥ 5	≥ 60°	4946	3274
≥ 10	≥ 75°	14767	286

III. DATA ANALYSIS

The procedure of reconstruction of local muon density distributions from the observed characteristics of muon bundles is started from the estimation of the parameters of a spectrum model in a following semi-empirical form:

$$dF_0(D,\theta)/dD = C\,D^{-(\beta+1)}\cos^{\alpha}\theta. \quad (1)$$

The parameters α,β are found by means of maximum likelihood method (on the event-by-event basis) for every experimental data sample. The distribution function of the coordinate detector response $P(m,\theta,\varphi;\alpha,\beta)$ for the above model of the spectrum is calculated taking into account the effective setup area $S(\theta,\varphi)$, Poisson fluctuations of the number of muons that hit the detector at a given density D, detection efficiency, triggering and selection conditions. Then the expected number of events with a given multiplicity in certain intervals of zenith and azimuth angles $N_{exp}(m,\Delta\theta,\Delta\varphi)$ is computed.

Finally, experimental estimates of the local muon density spectra are calculated as the ratios of the observed N_{obs} and expected N_{exp} numbers of the events in a given angular bin,

multiplied by the model spectrum (1) with best-fit parameters, which thus serves as a first iteration for the deconvolution:

$$dF(D,\theta)/dD = [dF_0(D,\theta)/dD] \times \times [N_{obs}(m,\Delta\theta,\Delta\varphi)/N_{exp}(m,\Delta\theta,\Delta\varphi)]. \quad (2)$$

The calculated dF/dD estimates are attributed to certain average values of zenith angle within the corresponding angular intervals and to the average muon density $\langle D \rangle$ of the events, contributing to the bundles with the observed multiplicity m. Taking into account Poisson fluctuations and the spectrum slope,

$$\langle D \rangle = (m - \beta) / S, \quad (3)$$

where S corresponds to the average detector area for a given angular range. A reasonable variation of the parameters α,β in Eq.(1) used as a first iteration for the deconvolution does not seriously influence the shape and absolute normalisation of the reconstructed spectrum (2), thus giving the evidence for the robustness of the applied procedure.

IV. Simulation details

At first, average muon LDF have been calculated. For that, simulation of EAS muon component by means of the CORSIKA code [5] (version 6.500) has been performed. Calculations have been done for fixed zenith angles (35°, 50°, 60°, 70°, 80° and 85°), a set of primary energies E (from 10^{14} to 10^{19} eV, one point per decade), pure protons and pure iron nuclei as primary particles. In present analysis, combination of hadronic models QGSJET01c + GHEISHA2002 is used; transition from high-energy interaction model (QGSJET) to the low-energy one (GHEISHA) is made at 80 GeV. Threshold energy of muons and hadrons is set as 2 GeV (close to average muon energy threshold in the experiment). For all variants (except 10^{18} and 10^{19} eV), the number of simulated events equals to 100; at highest energies, 50 and 20 proton showers, and 20 and 5 showers initiated by iron nuclei have been simulated.

Calculations have been performed in two versions: with consideration of the Earth magnetic field and without it. Main features of the EMF influence on EAS muon component were discussed in [8]. Due to a long distance from muon generation point to observation level, low energy muons are swept out to shower periphery; muons of higher energies are separated in sign and momentum. As a result, the axial symmetry of LDF is destroyed; muon density in the central part of the shower significantly decreases. The influence of this effect rapidly increases with zenith angle, since the magnetic displacement of particles is proportional to the squared geometrical path.

Particle coordinates given in the CORSIKA output file are re-calculated to a plane orthogonal to the shower axis, and average LDFs $\rho(E,\mathbf{r})$ with a logarithmic step in two coordinates (one of them parallel to the Lorentz force vector, and another one orthogonal to it) are constructed.

Local muon density spectra at different zenith angles are calculated by means of a convolution with the primary spectrum. As a model of the primary flux, a power type all-particle differential spectrum in the form $dN/dE = 5.0 \times (E, \text{GeV})^{-2.7}$ cm^{-2} s^{-1} sr^{-1} GeV^{-1} below the knee energy (4 PeV), steepening to $(\gamma + 1) = 3.1$ above the knee, is used. This spectrum is close to MSU spectrum [9] as given in [10], it is not very much different from the Akeno data [11] around the knee, and is in a reasonable agreement with Fly's Eye "stereo" results [12] around 10^{18} eV. To check the sensitivity of the experiment at highest energies, calculations with the ankle at 3 EeV have been also performed. As limiting cases of primary composition, pure proton and pure iron flux are considered.

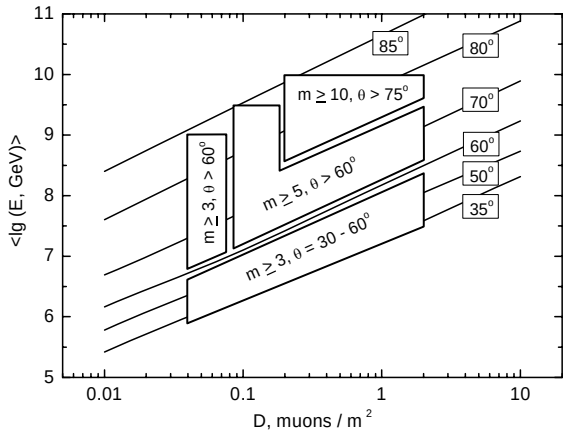

Figure 3. Average logarithms of primary energies, responsible for events with local muon density D, for various zenith angles (see the text for details).

In Fig.3, results of calculations of the average logarithms of the energy of primary particles that give contribution to events with a given local muon density D for several zenith angles (labels near the curves) are presented. The polygons in the figure outline the regions corresponding to selection of muon bundles of different categories (see Table I). The lower limit of accessible primary energies corresponds to about 10^{15} eV because of low muon densities in such EAS. On the other hand, statistical limitations appear around 10^{19} eV, since the total number of detected events with such muon densities and angles becomes low.

V. Results and discussion

The measured and calculated differential local muon density spectra for zenith angles 35°, 50°, 70°, and 80° are presented in Fig. 4. For the convenience of representation, spectra are multiplied by D^3. The points in the figure are obtained from different sub-sets of the experimental data (Table I); only statistical errors are shown. The curves correspond to calculation results for two versions of primary composition (only protons and only iron) with consideration of the influence of the Earth magnetic field.

A reasonable agreement (including the absolute normalisation) of the present data with CORSIKA-based simulation is observed. At moderate zenith angles, the steepening of the spectra related with the knee is seen. Large multiplicity events in the last angular interval, around 80° (bottom line in Table I), correspond to energy range $10^{18} - 10^{19}$ eV. Though statistics are limited, a flattening of the muon density spectrum (probably related with the ankle in the primary spectrum) is seen. Data for 70° correspond to intermediate primary energies (about 30 – 1000 PeV).

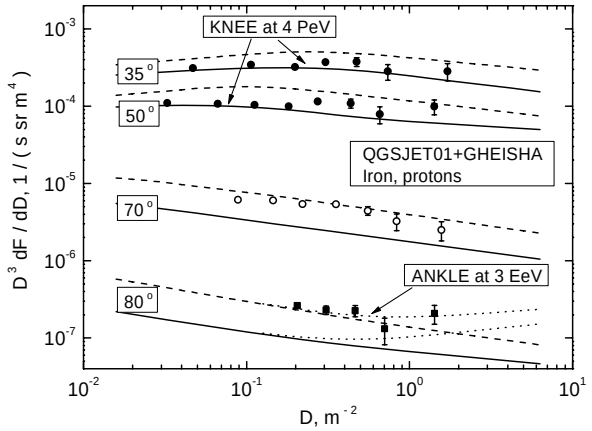

Figure 4. Differential spectra of local muon density for several zenith angles. Points represent different samples of the experimental data; curves are calculation results (dashed and solid curves correspond to primary iron nuclei and protons, respectively). Dotted curves for 80° reflect the expected influence of the ankle.

In Fig.5, zenith angular distribution of the events with local muon density exceeding a fixed threshold ($D > 0.04$ muons/m^2) is presented as a function of zenith angle cosine (log scale). For comparison, calculation results are presented for two versions: with consideration of EMF effect and without it. Difference between these two calculations increases with zenith angle, and at 80 – 85° exceeds the order of magnitude. Experimental data are in agreement with simulation including EMF. Remarkably, experimental points in Fig.5 lie near a straight line, thus indicating power law dependence of the intensity on cosθ.

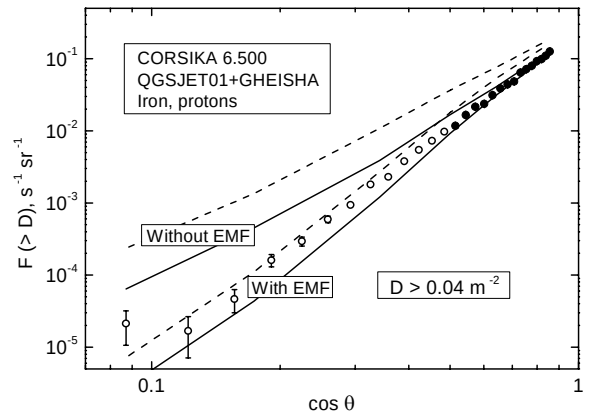

Figure 5. Zenith angle dependence of integral intensity for $D \geq 0.04$ muons/m^2. Points correspond to sub-sets of present data; curves are calculation results with consideration of EMF effect and without it. Notations are the same as in Fig.4.

In Fig.6, angular dependences of the intensity for several threshold densities are compared with simulation results; all the curves have been calculated with EMF. Both data and calculations in the figure are divided by a phenomenological factor $\cos^{4.5}\theta$. Within the experimental errors, data for different thresholds exhibit similar zenith angle dependence.

At first sight, comparison of the curves and the data in Fig.4 and Fig.6 evidences for an increase of the effective mass of primary particles with the increase of energy. It should be stressed however, that all simulations presented here have been performed for a fixed model of the primary spectrum (Section IV), and changes of its slope and normalization can significantly change the relation between data and the expectation. Besides, it is necessary to bear in mind also the existing uncertainties in hadronic interaction models at ultra-high energies.

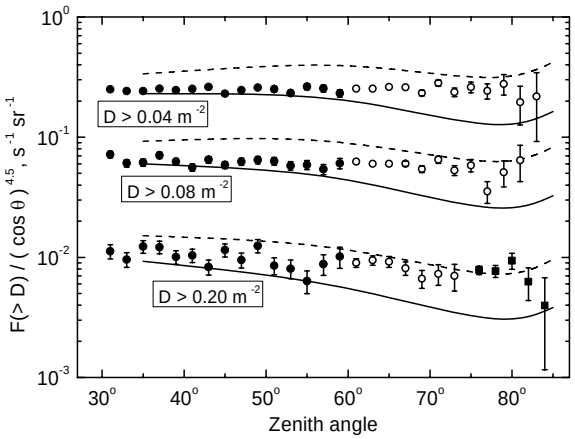

Figure 6. Zenith angular dependence of integral flux of events for several threshold local muon densities. Notations are the same as in Fig.4.

VI. Conclusions

Analysis of muon bundle events detected at experimental complex NEVOD-DECOR in frame of the approach based on a new phenomenological variable – local muon density – has shown that it is possible to investigate characteristics of primary cosmic ray flux in a very wide energy range (from the knee to the ankle) by means of a single detector of relatively small area. Local muon density distributions are sensitive to the shape of the primary spectrum and primary composition. Comparison of the measured local muon density spectra with CORSIKA-based simulations performed with consideration of the Earth magnetic field effects exhibits a reasonable agreement of data with the expectation. For quantitative conclusions, extension of the set of primary flux and hadronic interaction models is required. Hopefully, a further analysis of the data including those of independent experiments will allow putting new constraints on cosmic ray flux characteristics. The experiment, data analysis and simulations are being continued.

References

[1] M.B. Amelchakov et al. Izv. RAN, Ser. Fiz., **66** (2002) 1611.
[2] M.B. Amelchakov et al., Proc. 27th ICRC, Hamburg, **3** (2001) 1267.
[3] I.I. Yashin et al., Proc. 29th ICRC, Pune, **6** (2005) 373.
[4] M.B.Amelchakov et al. Presented at NANP'05, Dubna, 2005. To be published in: Phys. Atom. Nucl., **70** (2007).
[5] D. Heck et al. Forschungszentrum Karlsruhe Report, FZKA 6019, Karlsruhe, 1998.
[6] V.M. Aynutdinov et al. Astrophysics and Space Science, **258** (1998) 105.
[7] V.M. Aynutdinov et al. Nucl. Phys. B (Proc. Suppl.), **75A** (1999) 318.
[8] M. Ave et al. Astroparticle Phys., **14** (2000) 19.
[9] Yu.A. Fomin et al., Proc. 22th ICRC, Dublin, **2** (1991) 85.
[10] S. Eidelman et al. (Particle Data Group). Phys. Lett., **B592** (2004) 1.
[11] M. Nagano et al. J. Phys., **G10** (1984) 1295.
[12] D.J. Bird et al. Astrophys. J., **424** (1994) 491.